

Quantum Information Systems: Using a Two-Spin System and Nuclear Magnetic Resonance

Suzannah Wood, Sean McKenna, John Klingner
Cornell College

December 21, 2011

1 Introduction

Information systems are an essential part of everyday life. Standard computers rely on the detection of charge to process information; quantum computers use quantum states to represent information[15]. There are a few different techniques that can be used to complete quantum computations, including ion-trap[3], quantum dots[1], and nuclear magnetic resonance (NMR) experiments. In the case of our work, we employed a commercially available Nuclear Magnetic Resonance device and a chemical system of isotopically enriched Carbon-13 chloroform.

2 Motivation

The potential power of quantum computing is based on the ability of quantum systems to be in a superposition of states. All the numbers represented by these states can be manipulated simultaneously; this demonstrates quantum computing capacity for parallelism. The idea of parallelism arises from breaking down a complex and computationally heavy problem so that many different computers can work on it at the same time. In quantum parallelism, the fact that a quantum system can be in a superposition of states means that the same computation can be done on all possible states at the same time, decreasing the number of needed computations from 2^n to n [9].

3 Theory

3.1 Nuclear Magnetic Resonance (NMR)

Nuclear magnetic resonance occurs when the intrinsic spin of a nucleus interacts with static and oscillating magnetic fields. This is a special case of resonance. In our work we used pulsed NMR; in this technique a short radio frequency (RF) pulse

is applied and a free induction decay (FID) is measured[15]. When this microwave pulse is exactly at resonance, it can induce rotations of nuclear spin.

Looking at magnetic resonance from a quantum mechanical perspective, the energy of a spin- $\frac{1}{2}$ system is described by equation 1, where \hat{H} is the Hamiltonian for the system, $\hat{\mu}$ is the magnetic moment, γ is the gyromagnetic ratio and \mathbf{B} is the magnetic field along the z-axis[13].

$$\hat{H} = \hat{\mu} \cdot \mathbf{B} = -\gamma B S_z \quad (1)$$

The probability of the particle being spin up or spin down does not vary with time, therefore spin up $|+\mathbf{z}\rangle$ and spin down $|-\mathbf{z}\rangle$ are stationary states of the Hamiltonian.

When an additional oscillating magnetic field is added to the system transverse to the z-axis (along the x-axis), the Hamiltonian for this system changes. The Hamiltonian for this system appears in equation 2, where ω_o is the Larmor frequency, g is the coupling constant related to the oscillating magnetic field, and \hat{S}_z and \hat{S}_x are the Pauli spin matrices[13].

$$\hat{H} = \hat{\mu} \cdot \mathbf{B} = \omega_o \hat{S}_z + g(\cos\omega t)\hat{S}_x \quad (2)$$

Transitions between the spin up $|+\mathbf{z}\rangle$ and spin down $|-\mathbf{z}\rangle$ states can occur by properly adjusting the frequency of this transverse field, i.e. meeting the resonance condition. For nuclei in atoms or molecules, the magnetic field B_o is a combination of the known externally applied field and the local magnetic field at the site of the nucleus, which is influenced by chemical bonds with neighboring atoms.

3.2 Quantum Computing and NMR

Nuclear Magnetic Resonance (NMR) approaches quantum computing from a macroscopic perspective, due to the fact there is a bulk ensemble of particles. The initial state of the entire system is a thermal

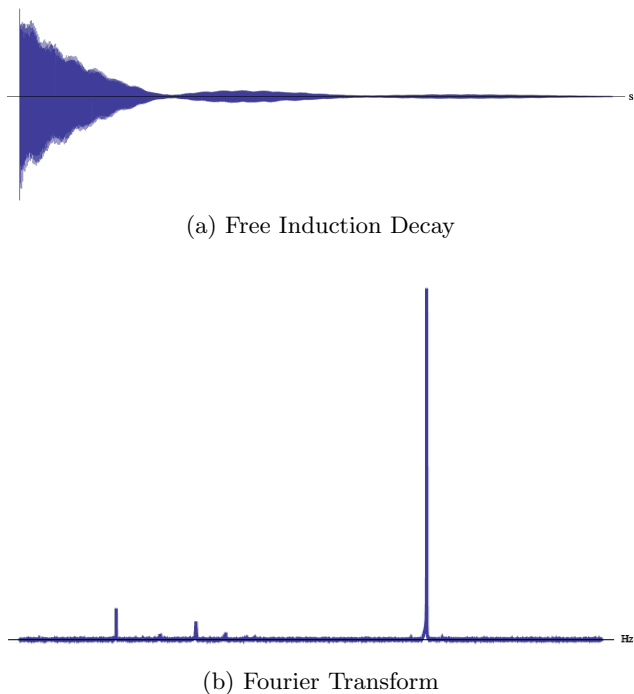


Figure 1: 7% by weight ^{13}C -Chloroform Solution, Raw FID and Spectra

state given by a Boltzmann distribution. This can be thought of as a bulk computation performed by a large ensemble of indistinguishable quantum computers. Each member of the ensemble has an initial state such that only the average of these states is known[8]. This average value of states is found from a Fourier transform of the free induction decay (FID). See Figure 1 for a sample FID and spectrum produced by a Fourier transform.

Rotations are single qubit operations [7]. Experimentally, rotations can be performed for any value of θ by controlling external magnetic fields about the x- and y- axis; this is done by controlling the RF-pulse. Any quantum logic gate can be composed by rotations and the controlled-NOT (c-NOT) gate [10].

The operation of a c-NOT gate can be described by the following: “if the first qubit is spin down, then flip the second qubit.” [11] The c-NOT gate is an important gate because it preserves the information of the previous state after being applied to a quantum state. This preservation of previous states allows for the computation to be reversible an essential property of quantum systems[4].

3.3 The Quantum System

The quantum system used in this experiment is isotopically enriched ^{13}C Chloroform ($^{13}\text{CHCl}_3$). This

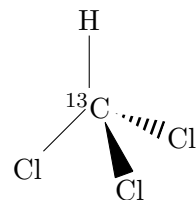


Figure 2: Carbon-13 Chloroform is a two spin system. ^{13}C has a spin of $\frac{1}{2}$. ^1H has a spin of $\frac{1}{2}$. The J-Coupling constant is approximately 215 HZ[10].

molecule is a two-spin system. The hydrogen (^1H) and the carbon-13 (^{13}C) nuclei have an intrinsic spin of $1/2$. The resonant frequency of a spin is intrinsic to a particular atomic nucleus, but is influenced by the chemical environment. Spins can be coupled by dipole coupling and through-bond coupling (J-coupling) [15]. J-Coupling is due to the fact that the magnetic field felt by one nucleus is perturbed through the overlap of its wavefunction with the other nucleus in the bond. J-Coupling is simplified in liquid phase NMR because the couplings are weak [15]. On average, the J-Coupling between a proton and the directly attached ^{13}C is between 125 and 200 Hz [12].

4 Sample Preparation

There are several things to consider when preparing an NMR sample. The first is concentration. Different concentrations are ideal for ^1H and ^{13}C NMR due to the fact that ^{13}C is about 6000 times less sensitive than ^1H at natural concentrations. If the sample is not concentrated enough, the spectral lines in the Fourier transform will be dominated by the lines of common contaminants such as water. If the sample is too concentrated, the increased viscosity of the solution will result in broad spectral lines[2]. The MIT junior lab suggested that the concentration of the samples should be seven percent by weight $^{13}\text{CHCl}_3$ with a solvent of D-6 Acetone[10].

D-6 Acetone is a common NMR solvent for several reasons. First, the signal of deuterium does not interfere with the ^1H response; if we were to use a solvent with a natural hydrogen abundance, the signal from the protons in the solvent would completely overwhelm and dominate the signal of the sample. Secondly, the deuterated solvent allows for a deuterium lock signal, which monitors the resonance frequency response of the deuterium and adjusts the magnetic field to keep that response constant.

Using a spreadsheet with the inputs of total de-

$$V_{^{13}\text{CHCl}_3} = \frac{V_{TOT} * \rho_{^{13}\text{CHCl}_3} * \alpha_{^{13}\text{CHCl}_3} * \rho_{\text{D-6 Acetone}}}{(\alpha_{^{13}\text{CHCl}_3} * \rho_{\text{D-6 Acetone}}) + (100 - \alpha_{^{13}\text{CHCl}_3}) * \rho_{^{13}\text{CHCl}_3}} \quad (3)$$

sired volume of the sample, the percent weight of the sample, and the densities of D-6 Acetone and $^{13}\text{CHCl}_3$, we calculated the desired volumes of the sample ($^{13}\text{CHCl}_3$) and the solvent (D-6 Acetone). Equation 3 is a sample calculation for the desired volume of ^{13}C -Chloroform given a desired total volume, where α is the percent by weight and ρ is the density. The volume of solvent required will simply be $V_{TOT} - V_{^{13}\text{CHCl}_3}$.

4.1 NMR Tube Preparation

To prepare the NMR tube for the sample, wash with acetone. Leave the NMR tube lying flat on its side in a fume hood for approximately 24 hours. Next, place the NMR tube into a desiccator for approximately 3 days, once again, lie flat. This procedure should be ample to completely evacuate the acetone vapor from the NMR tube.

4.2 Sample Preparation

Use the NMR tube prepped by the method above to prepare your sample for the NMR. Carefully measure out the correct volume of $^{13}\text{CHCl}_3$ using a syringe that has been washed and prepped in the same method as the NMR tube, and insert the chloroform into the NMR tube. Next, using another syringe prepared using the same method, measure out the D-6 Acetone and place into the NMR tube with the $^{13}\text{CHCl}_3$. Cap the tube and turn over about a dozen times to completely mix the sample and the solvent. Insert the capped NMR tube into the NMR spinner and place into the NMR device.

We prepared a seven percent by weight $0.500 \pm 0.005_3$ mL sample, with 0.021 ± 0.002 mL of $^{13}\text{CHCl}_3$ and 0.479 ± 0.005 mL of D-6 Acetone.

5 Equipment

The spectra were collected using a JEOL Eclipse 270 MHz spectrometer. We used Delta version 4.3.6 for data collection; this software both interfaced with and controlled the NMR device and collected spectra. We used Delta version 4.3.6, Wolfram Mathematica 8, and ACD/Labs Software, version 12.00 for data processing.

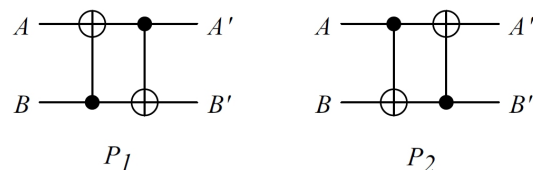


Figure 3: Quantum circuit implementation of the experiments P₁ and P₂ for temporal averaging via exhaustive averaging. \oplus is the controlled not gate. \bullet represents the control bit. A and B represent the two different qubits [8].

6 Pulse Programming

The most difficult and time consuming part of our work was pulse programming. Different pulse widths and delay times manipulate the sample in different ways [10]. Pulse width corresponds to the length of the radio frequency pulse. The delay time is the time between pulses.

6.1 Creating an Effective Pure State by Temporal Averaging

In order to implement a logic gate, we need to know the initial state of the system and how that state transforms when a logic gate is applied. Ideally, we would implement a logic gate on a pure state, such as what would exist at 0 Kelvin. However, these experiments are done at room temperature and the initial spin state of the system is almost completely random (in reality it is given by a Boltzmann distribution), so the next best alternative is an effective pure state. Effective pure states allow for the dynamics of a 0 Kelvin system to be observed even at high temperatures, or in our case room temperature[10].

In the case of our work, we prepared an effective pure state using the method of temporal averaging by the exhaustive averaging technique. This technique is reasonably implemented on a 2-qubit system, requiring only three experiments. The first two of these experiments are implemented using a controlled-NOT gate, the quantum circuit diagram is shown in figure 3. This diagram suggests that a controlled-NOT gate will be implemented on one qubit while the other is held constant and then vice versa. Figure 4 shows the corresponding pulse

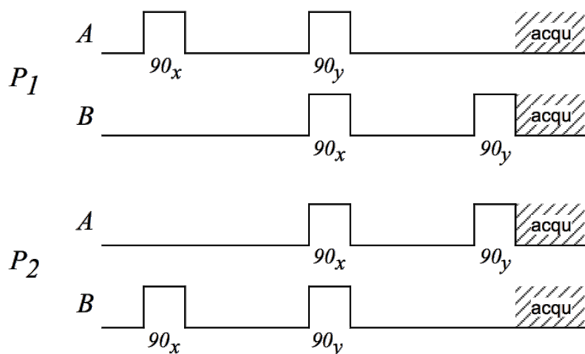


Figure 4: The pulse chart for experiments P_1 and P_2 for temporal averaging via exhaustive averaging. A and B represent the two different qubits. The pulse widths are approximately $10 \mu\text{s}$ and the delay times are approximately 2.3 ms [8].

charts. The pulse charts show what length and frequency pulse we implemented for P_1 and P_2 as well as the delay times between the pulses, where P_1 and P_2 represent experiments 1 and 2 of the exhaustive average. These figures are from E. Knill’s paper, refer to reference [8]. The third experiment is simply a reading of the thermal state. The pulse chart for P_1 using our delta software does not correspond perfectly to the pulse chart in Figure 4. The translation between the different representations of the pulse sequence was where we did the bulk of our work. An additional complication was that literature pulse chart were not always consistent (refer to references [6] and [12] for an example of this inconsistency).

We set the domain of our spectrometer to proton, in order to collect hydrogen spectra. We centered the spectra at the midpoint of the two hydrogen lines, 2150.620 Hz . We collect spectral data for a range of 430.528 Hz , which is double the J-Coupling constant. We scanned the sample four times for one free induction decay; the free induction decay of each sample was added to the previously taken scans in order to eliminate machine noise, which is assumed to be random. Spin A (Qubit A) corresponds to hydrogen and qubit B corresponds to carbon. The hydrogen 90_x pulse is $9.8 \mu\text{s}$ long; the carbon 90_x pulse is $8.8 \mu\text{s}$ long. The 90_y pulses are the same length as the 90_x pulses but occur at a different axis; the delay between pulses was 2.3 milliseconds . In the Delta software we were able to specify all these parameters in the experiment file. The experiment file is where we designed pulses.

In		Out	
A	B	A	B
0	0	0	0
0	1	0	1
1	0	1	1
1	1	1	0

Figure 5: Truth Table for C-Not Gate

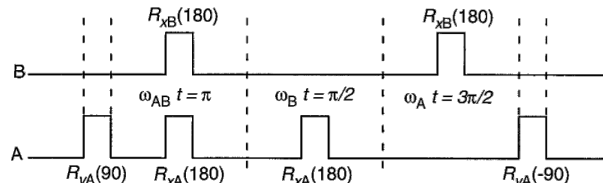


Figure 6: Controlled-NOT gate pulse chart, as seen in Reference [5]. The 180_x pulses are twice the length of 90_x pulse length.

6.2 Creating the Four Input States

In order to prepare the four effective pure spin energy states, we implemented a NOT gate in two different ways. To NOT the carbon qubit, we simply sent a 180_x carbon pulse which is twice the pulse length of a 90_x carbon pulse. To NOT the hydrogen qubit, we implemented a DEPT pulse. We choose to implement a DEPT pulse because it the equivalent of a NOT gate[6]. Reference [6] does not provide a DEPT pulse sequence for carbon, thus we choose to use a 180_x carbon pulse. By "NOT-ing" the appropriate qubit, we were able to prepare all four input states necessary to test a classical logic gate.

6.3 Implementation of the c-NOT Gate

Using the four prepared input states, we attempted to implement a c-NOT gate, and confirm its classical truth table, see Figure 5. Recall, the c-NOT gate flips the second qubit, if the first qubit is one. The c-NOT gate pulse chart is shown in Figure 6. The pulses are denoted differently in this chart. $R_y(90)$ is an equivalent pulse to a 90_y pulse. The 180_x pulses are twice the length of 90_x pulse length. Also note, that the hydrogen qubit is on the bottom and the carbon qubit is on the top. Due to the fact that this implementing this gate was the last thing we worked on this block we were not able to fully troubleshoot it, or fully confirm its classical truth table.

7 Data Collection and Analysis

We controlled the spectrometer and sent pulses using Delta version 4.3.6. This program also collected the free induction decays and performed the Fourier transform. The program also had the option of machine phasing however we decided not to adjust the phase of our spectra in the analysis and leave the phase of the spectra as it stood when collected. We decided to do this because the machine phasing seemed almost arbitrary and we wanted all three experiments used in temporal averaging to be the same phase when averaged together. The spectral data was exported as a text file from the Delta software to Mathematica. In Mathematica each Fourier transform was normalized so that the highest peak was equal to one and then processed to make the semi-pure state. Figure 7 shows the three experiments that when averaged together form our effective pure state. The first two states are described in figures 3 and 4. The third state is the thermal state, which displays the population states populated at room temperature. The final spectra were plotted using mathematics and the integrals of the peaks could be calculated using ACD/Labs Software, version 12.00. The integration is important because area of the peak is a function of the spin state[10].

8 Results

8.1 The Four Spin Energy States

The four input states are shown in Figure 8. The preparation of these for states is important building block for quantum computation, because in order to test a classical truth table for a logic gate a pure or an effectively pure state must exist for each possible input into that gate.

The first input state shown in Figure 8 is simply the effective pure state whose preparation was described above. This state corresponds to the $\uparrow\uparrow$ or 00; this state is the ground state of the system where both the ^1H and ^{13}C spins are aligned with the static magnetic field. The peak in the hydrogen spectra is pointing up and is on the left. The placement of one spin in the spectrum indicates the state of the other spin[14]. The peak itself describes the state of the hydrogen spin (qubit); the placement of this peak on the left side of the spectra indicates that carbon is also aligned with static magnetic field.

The second state shown in Figure 8 is the $\uparrow\downarrow$ or 01 state. This state is prepared by "NOT-ing", i.e.

flipping, the hydrogen qubit while leaving the carbon qubit alone. This is the second highest energy state. In this spin energy state, the spin of carbon is aligned with the static magnetic field and the spin of hydrogen is aligned against the static magnetic field. The peak on the left indicating that the carbon qubit is $|0\rangle$; the peak is down indicating that the hydrogen qubit is $|1\rangle$.

The third state shown in Figure 8 is the $\downarrow\uparrow$ or 10 state, which is prepared by "NOT-ing" the carbon qubit while leaving the hydrogen qubit alone. This state is the second lowest energy state. In this state, the spin of hydrogen is aligned with the static magnetic field and the spin of carbon is aligned against the static magnetic field. The peak on the right indicating that the carbon qubit is $|1\rangle$; the peak is up indicating that the hydrogen qubit is $|0\rangle$.

The final of the four input states, shown in Figure 8 is prepared by simultaneously "NOT-ing" both the carbon and hydrogen qubits. This is the highest energy state; in this state both the hydrogen and carbon spins are aligned against the static magnetic field. The peak on the right indicating that the carbon qubit is $|1\rangle$; the peak is down indicating that the hydrogen qubit is $|1\rangle$. Although, the relative magnitude of the peak height may seem incorrect, the input states are not as bad as they appear. When you take the integral of the peaks, the area of the peak on the left is approximately five times less than the one on the right.

8.2 Implementation of c-NOT Gate

Figure 9 shows the results of our attempt to implement the c-NOT gate to the four input states. In this figure, the input state is in blue; the output state is in red. The c-NOT gate worked as expected for the input: $\uparrow\uparrow$ or 00, $\uparrow\downarrow$ or 01, and $\downarrow\downarrow$ or 11. However, we got the same input as output for the input state $\downarrow\uparrow$ or 10. We expected to get the state $\downarrow\downarrow$ or 11 as the output; this did not occur.

9 Conclusions and Future Work

Our work demonstrated the ability for quantum computations at Cornell College using the technique of nuclear magnetic resonance. We were able to successfully prepare a effective pure state, using temporal averaging. Using a NOT gate we were able to prepare the four input states that are necessary to confirm the classical truth table for a c-NOT gate. We were able to implement a c-NOT gate on the input

states with some, but not complete, success. Future work includes: a successful implementation of a c-NOT gate on the input states; a systematic study of pulse sequences in order to more completely understand, and more simply implement pulse sequences; running quantum algorithms[10][15]; and expanding to a chemical system with more qubits.

References

- [1] Supriyo Bandyopadhyay and Vwani Roychowdhury. Computational paradigms in nanoelectronics: Quantum coupled single electron logic and neuromorphic networks. *Japanese Journal of Applied Physics*, 35(Part 1, No. 6A):3350–3362, 1996.
- [2] Alan S.F. Boyd. How to prepare samples for nmr.
- [3] J. I. Cirac and P. Zoller. Quantum computations with cold trapped ions. *Phys. Rev. Lett.*, 74:4091–4094, May 1995.
- [4] David G. Cory, Amr F. Fahmy, and Timothy F. Havel. Ensemble quantum computing by nmr spectroscopy. *Proceedings of the National Academy of Sciences*, 94(5):1634–1639, 1997.
- [5] Neil A. Gershenfeld and Isaac L. Chuang. Bulk spin-resonance quantum computation. *Science*, 275(5298):350–356, 1997.
- [6] A. Güleç and S. Bahçeli. "quantum gates based on polarization transfer nmr spectroscopy". *Acta Physica Polonica A*, 107:983, June 2005.
- [7] J. A. Jones. Nmr quantum computation. *Chem-Inform*, 32(29):288–288, 2001.
- [8] E. Knill, I. Chuang, and R. Laflamme. Effective pure states for bulk quantum computation. *Phys. Rev. A*, 57:3348–3363, May 1998.
- [9] Shu-Shen Li, Gui-Lu Long, Feng-Shan Bai, Song-Lin Feng, and Hou-Zhi Zheng. Quantum computing. *Proceedings of the National Academy of Sciences*, 98(21):11847–11848, 2001.
- [10] MIT Department of Physics. Quantum information processing with nmr. August 2010.
- [11] D. Cory E. M. Fortunato T. F. Havel C. Miquel R. Martinez C. J. Negrevergne G. Ortiz M. A. Pravia Y. Sharf S. Sinha R. Somma L. Viola R. Laflamme, E. Knill. Nmr and quantum information processing. *Los Alamos Science*, (27):226–259, 2002.
- [12] John D. Roberts. *ABCs of FT-NMR*. University Science Books, 2000.
- [13] John S. Townsend. *A Modern Approach To Quantum Mechanics*. McGraw-Hill, 1992.
- [14] Lieven M. K. Vandersypen, Isaac L. Chuang, and Dieter Suter. *Liquid-State NMR Quantum Computing*. John Wiley & Sons, Ltd, 2007.
- [15] Vorlesung. *NMR Quantum Computing*, pages pp. 83–115.

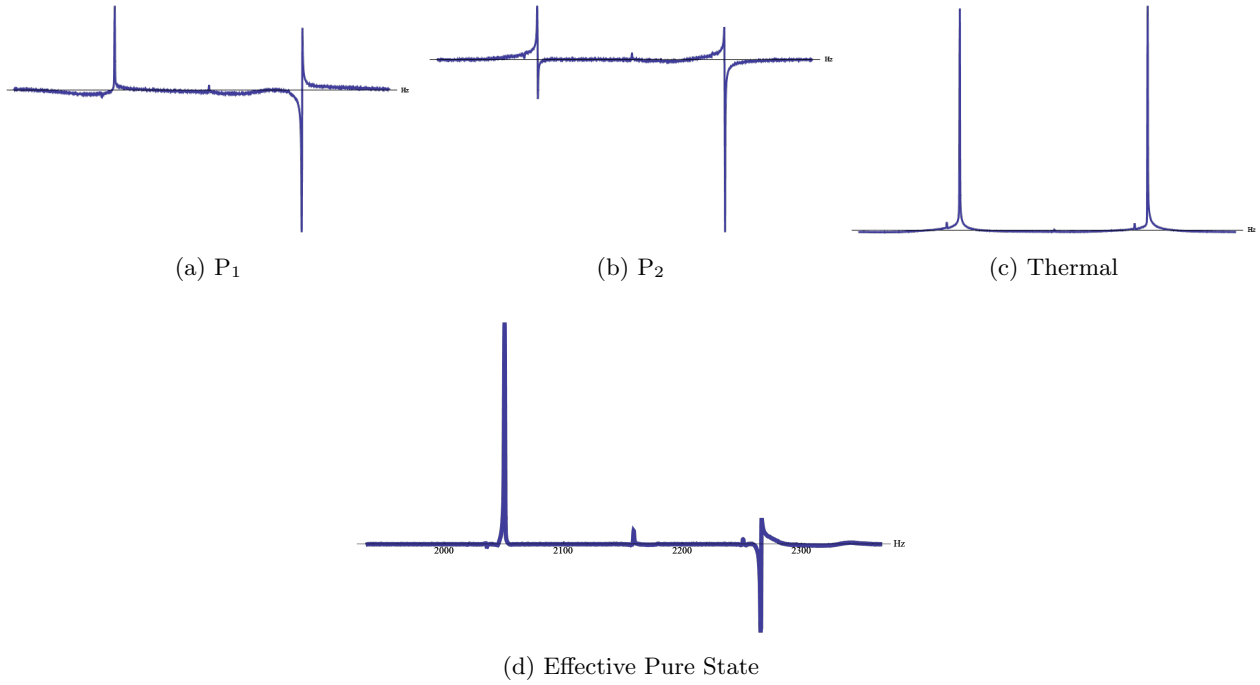


Figure 7: Results of the three experiments for and their average, our Effective Pure State

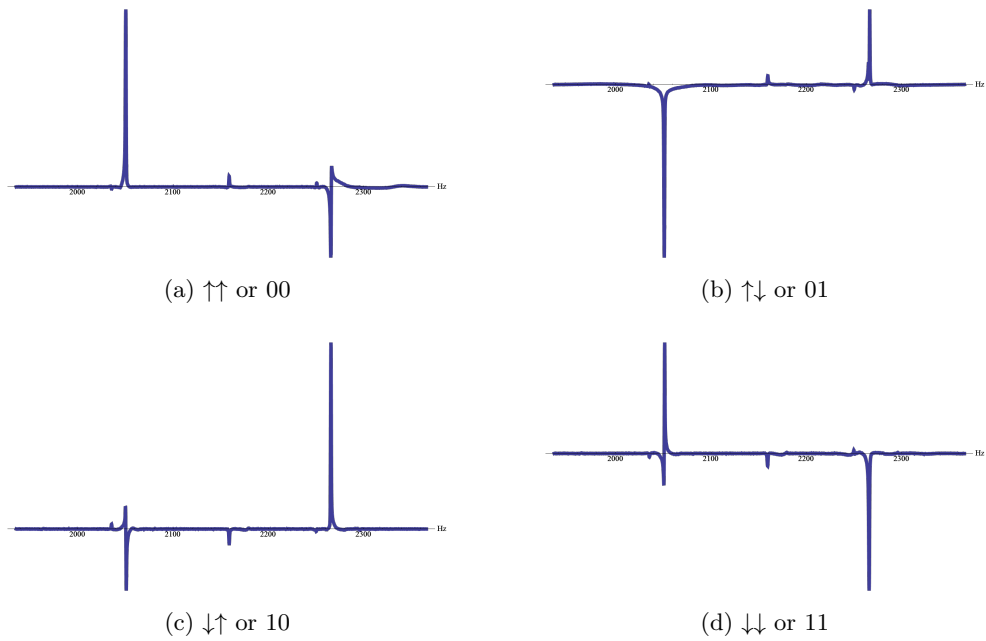


Figure 8: The four prepared input states.

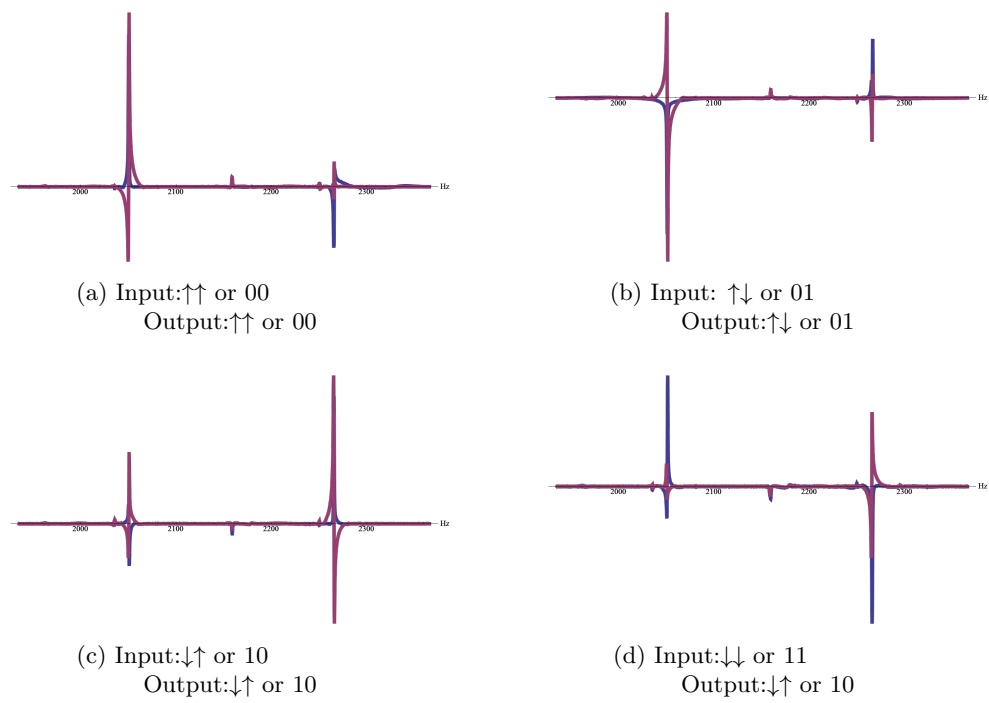


Figure 9: Result of Implementing the c-NOT gate to the four input states. The input state is in blue; the output state is in red.